Explosive transitions in coupled Lorenz oscillators

Yusra Ahmed Muthanna [1,2] and Haider Hasan Jafri [1]
[1] *Department of Physics, Aligarh Muslim University, Aligarh 202 002, India*
[2] *Physics Department, Taiz University, Taiz 6803, Yemen*

(Received 5 December 2023; accepted 16 April 2024; published 16 May 2024)

We study the transition to synchronization in an ensemble of chaotic oscillators that are interacting on a star network. These oscillators possess an invariant symmetry and we study emergent behavior by introducing the timescale variations in the dynamics of the nodes and the hub. If the coupling preserves the symmetry, the ensemble exhibits consecutive explosive transitions, each one associated with a hysteresis. The first transition is the explosive synchronization from a desynchronized state to a synchronized state which occurs discontinuously with the formation of intermediate clusters. These clusters appear because of the driving-induced multistability and the resulting attractors exhibit intermittent synchrony (antisynchrony). The second transition is the explosive death that occurs as a result of stabilization of the stable fixed points. However, if the symmetry is not preserved, the system again makes a first-order transition from an oscillatory state to death, namely, an explosive death. These transitions are studied with the help of the master stability functions, Lyapunov exponents, and the stability analysis.

DOI: 10.1103/PhysRevE.109.054206

I. INTRODUCTION

Coupled nonlinear oscillators serve as an excellent tool to study the spontaneous emergence of collective behavior in many complex systems in nature. Depending upon the nature of coupling, properties of the isolated units and the coupling topology, the ensemble may exhibit a plethora of phenomenon, namely, synchronization, clusters, and chimera states [1,2]. Synchronization is an important collective behavior observed in nature, social science, and engineering [1,3]. Such an onset of coherence in real systems has been reported in power grids, neuronal networks, communication networks, and circadian rhythm [1]. Most studies suggest that this transition from desynchrony to synchrony is second order in nature. This is characterized by an order parameter that shows a smooth transition as the coupling strength is varied. However, recently it has been reported that a first-order transition from desynchrony to synchrony, namely, explosive synchronization (ES), where the order parameter changes abruptly, may also occur. This transition is associated with a hysteresis when the coupling strength varies gradually in the forward and backward directions. This transition, reported by Gómez-Gardeñes *et al.* in a scale-free network [4], occurs because of the positive correlation between the oscillator's natural frequency and its degree. Another emergent phenomenon, as a consequence of coupling in an ensemble of coupled oscillators, is the suppression of oscillations or oscillation quenching, which is called an explosive death (ED) [5–7]. It was shown that ED is a first-order and irreversible transition where the emergent dynamics is a steady state resulting in complete suppression of oscillations [5,8].

Since the discovery of ES, various techniques have been introduced to induce the first-order transition to synchrony in the network [9]. Such a transition to synchrony was observed in the case of second-order Kuramoto oscillators, where inertia plays an important role [10]. In a separate study, it was shown that it is possible to observe ES in networks having a time delay [11]. It has been observed that ES occurs in various real-world networks [12] ranging from brain convulsions caused by epilepsy [13], fibromyalgia brain [14], power grid failures cascading [15], and internet jamming [16].

When the node dynamics is a second-order Kuramoto oscillator, the transition to synchrony takes place via the abrupt formation of the intermediate clusters, a phenomenon known as cluster explosive synchronization [17]. Recently, it was demonstrated that ES can also be observed in multilayer networks under a variety of circumstances, including interlayer coupling [18,19], inertia [20], and connection with inhibitory layers [21]. It was shown that in the presence of interlayer coupling, it is possible to achieve successive explosive transitions, namely, double explosive transitions [22].

Most studies on explosive transitions have focused on the oscillators having phase dynamics, namely, the Kuramoto oscillators or periodic dynamics, e.g., the Stuart-Landau oscillators [4,23–25], except for a few cases where this transition has been observed in coupled chaotic oscillators [26–28]. A paradigmatic model to study chaotic systems in nonlinear dynamics that has been used for decades now is the Lorenz system [29]. This system has been useful to mimic various scenarios that are physically useful such as convection rolls in atmosphere [30], single mode lasers [31], and segmented disk dynamos [32], and, therefore, has been used to study chaos synchronization in such systems.

In nature, networks are usually heterogeneous and may have scale-free topology where some dynamical units hold a large number of connections. The star networks—with a central node having high connections along with low-degree peripheral nodes—are typically used to represent the hub structure observed in these networks. Therefore, star topology can be considered the building blocks of scale-free networks.

To understand the interaction between network structure and the dynamics of the individual units, the oscillator frequencies can be considered to be correlated with some network (topological) property (in this case, the degree). Such correlated dynamics can be observed in, for example, power grid networks where more nodes are connected to the hub node with more power, and the grid frequency of the hub varies according to the load [33–35]. In demand-supply networks, the hubs are typically the nodes with more mass or information as compared to other nodes. The neural network of the worm *Caenorhabditis elegans* is an explicit example where partial degree-frequency correlation leads to explosive synchronization [36]. Such degree-frequency correlation may lead to enhanced synchronizability [37] or lead the system to exhibit an explosive (first-order) synchronization transition [4]. Exploring emergent dynamics on networks having degree-frequency correlation gives fundamental insight into how individual elements interact within a structured environment, providing the motivation to study dynamical systems in such a specific setup. To incorporate this effect, we introduce variations in the timescales of the interacting units as described in Refs. [26,38].

In this paper, we give evidence to show that multiple explosive transitions, each having its own hysteresis loop, can take place in a system of coupled chaotic oscillators. We consider a star network where the dynamics on each node is that of a Lorenz oscillator that belongs to an essential class of chaotic systems having inherent symmetries. These symmetries may either be preserved or destroyed in the presence of coupling. We explore the dynamical consequences of preserving and breaking the symmetry in a network of coupled Lorenz oscillators. If the coupling is done in such a way that it preserves symmetry, the system shows consecutive explosive transitions, each with its own hysteresis region. For small coupling values, the first transition is an irreversible transition to synchronization, namely, explosive synchronization. As the coupling strength increases, a second irreversible transition from the synchronized oscillatory state to a steady state, namely, explosive death takes place. This system-specific double transition adds a fresh perspective to the study of explosive transitions. We note that the first transition takes place in small steps through the formation of clusters. This is due to the fact that in the presence of coupling, multistability is induced in the system [39–41]. These multistable attractors exhibiting intermittent synchrony (desynchrony) are responsible for the formation of clusters. This transition is irreversible in the sense that, if the coupling strength is decreased adiabatically, the system shows an abrupt transition to desynchrony at a different value of coupling strength. This results in a well-defined hysteresis. However, if the coupling is done so as to break the symmetry, we again observe an abrupt transition to the steady state, i.e., explosive death. We observe that the coupling strength and the mismatch in the timescale of the oscillators on the nodes and the hub play a crucial role in defining these transitions.

This paper is organized as follows: In Sec. II, we consider the Lorenz oscillators coupled in a star network configuration. We examine the impact of symmetry-preserving coupling and demonstrate the existence of ES in Sec. III. In Sec. IV, we take into account the symmetry-breaking situation and discuss various dynamical regimes. Finally, we summarize our results in Sec. V.

II. MODEL

In this paper, we consider coupled Lorenz oscillators on a star network and examine the emergent dynamics in the system. The star network configuration is described by N nodes connected to a single central hub. The equations of motion for the dynamics on the nodes is given by

$$\begin{aligned}\dot{x}_i &= \alpha_n[\rho(y_i - x_i) + \varepsilon_x(x_h - x_i)],\\ \dot{y}_i &= \alpha_n[\gamma_n x_i - y_i - x_i z_i + \varepsilon_y(y_h - y_i)],\\ \dot{z}_i &= \alpha_n[x_i y_i - \beta z_i + \varepsilon_z(z_h - z_i)],\end{aligned} \tag{1}$$

and the dynamics of the hub is given by

$$\begin{aligned}\dot{x}_h &= \alpha_h\left[\rho(y_h - x_h) + \frac{\varepsilon_x}{N-1}\sum_{i=1}^{N-1}(x_i - x_h)\right],\\ \dot{y}_h &= \alpha_h\left[\gamma_h x_h - y_h - x_h z_h + \frac{\varepsilon_y}{N-1}\sum_{i=1}^{N-1}(y_i - y_h)\right],\\ \dot{z}_h &= \alpha_h\left[x_h y_h - \beta z_h + \frac{\varepsilon_z}{N-1}\sum_{i=1}^{N-1}(z_i - z_h)\right],\end{aligned} \tag{2}$$

where the subscript $i = 1, \ldots, N$ labels the variable of the oscillators on the nodes and subscript h describes the variables of the hub. The Lorenz system in the uncoupled case exhibits three steady states, namely, $P_0 = (x_0^*, y_0^*, z_0^*) = (0, 0, 0)$ and $P_\pm = (x_\pm^*, y_\pm^*, z_\pm^*) = (\pm\sqrt{\beta(\gamma-1)}, \pm\sqrt{\beta(\gamma-1)}, \gamma - 1)$. For $\gamma < 1$, only P_0 is stable, which loses its stability at $\gamma = 1$, giving birth to two stable fixed points, $P_\pm$. For the parameter values $\gamma > 1$, all three equilibrium points remain stable until $1 < \gamma < \gamma_c$, where γ_c denotes the critical parameter given by $\gamma_c = \frac{\rho(\rho+\beta+3)}{\rho-\beta-1} = 24.74$. We consider the system parameters to be $\rho = 10$, $\gamma_n = 28$, and $\gamma_h = 30$, $\beta = 8/3$ such that the uncoupled systems exhibit chaotic dynamics. Timescale parameters α_n and α_h have been introduced to adjust the natural frequency of the oscillator as described in Ref. [38]. In this way, we ensure degree-frequency correlation by setting $\alpha_n = 2$ and $\alpha_h = 20$. The coupling strength in variables x, y, and z is given by ε_x, ε_y, and ε_z, respectively. Under the transformation $(x, y, z) \to (-x, -y, z)$, the system remains invariant. Therefore, coupling in the z variable, namely, $\varepsilon_x = \varepsilon_y = 0$, $\varepsilon_z \neq 0$ preserves symmetry. Alternately, for $\varepsilon_z = 0$ and $\varepsilon_x \neq 0$ or $\varepsilon_y \neq 0$, symmetry is not preserved [40–42]. We consider the interactions for which the oscillators are connected through one variable only. Clearly, they can be connected in a way that either the symmetry is intact or is destroyed. Note that the Lorenz attractor has two rotation centers, therefore, it is convenient to define the phase in the $u - z$ plane, where $u_i = \sqrt{x_i^2 + y_i^2}$. The instantaneous phase for the ith oscillator is thus given by $\phi_i(t) = \arctan[(u_i(t) - u^*)/(z_i(t) - z^*)]$, where $u^* = \sqrt{x^{*2} + y^{*2}}$. x^*, y^*, z^* are the equilibrium points P_0 or $P_\pm$ denoting the rotation centers of the attractors. Thus, by defining a universal order parameter, we can calculate the

average degree of the phase synchronization as

$$R = \left\langle \left| \frac{1}{N} \sum_{j=1}^{N} e^{i\phi_j(t)} \right| \right\rangle_t, \tag{3}$$

where $|\,.\,|$ denotes the modulus and $<\,.\,>$ represents the time average. When R is small ($R \sim 0$), the oscillators' phases are dispersed randomly across a unit circle, and the state is desynchronized; nevertheless, when R is large ($R \sim 1$), phase synchronization occurs. Throughout the investigation, the fourth-order Runge-Kutta method with step size $dt = 0.001$ is used to solve the differential equations. By varying the coupling strength adiabatically, the order parameter R is assessed in both forward and backward directions. For forward transitions, we begin with random initial conditions and increase the coupling parameter. The final state serves as the initial condition for the coupling parameter's subsequent value. For the backward transition, we choose the initial condition of a coherent state and adiabatically reduce the coupling strength. For each value of the coupling strength, we start with initial conditions that are very close to the coherent state.

Further, to study the transition to explosive death, an order parameter based on the average amplitude may be defined, namely,

$$a(\varepsilon) = \frac{1}{N} \sum_{i=1}^{N} [\langle x_{i,\max} \rangle_t - \langle x_{i,\min} \rangle_t], \tag{4}$$

where $\langle x_{i,\max} \rangle_t$ and $\langle x_{i,\min} \rangle_t$ represents the global maximum and minimum values of the time series of the ith oscillator. The normalized average amplitude of all the oscillators can be written as

$$A(\varepsilon) = \frac{a(\varepsilon)}{a(0)}. \tag{5}$$

If the dynamics is oscillatory, $A(\varepsilon)$ is nonzero, whereas if the system is in a steady state, $A(\varepsilon) = 0$.

III. DYNAMICAL TRANSITIONS IN SYMMETRY PRESERVING CASE

We consider a star network of nonidentical chaotic Lorenz oscillators described by Eqs. (1) and (2). To preserve symmetry, we consider $\varepsilon_x = \varepsilon_y = 0$ and vary the coupling strength ε_z. We observe that for different ranges of ε_z values, the system shows two different transitions. In the range $0 < \varepsilon_z < 0.35$, the system shows an explosive transition to synchronization as shown in Fig. 1(a). For the coupling strength $\varepsilon_z \geqslant 0.35$, we observe an abrupt transition to the steady state described in Fig. 1(b). We shall discuss each of these transitions as follows.

A. Transition to synchronization ($0 < \varepsilon_z < 0.35$)

As shown in Fig. 1(a), we observe two sharp transitions from desynchronized state ($R \approx 0$) to synchrony ($R = 1$) in the forward direction and vice versa in the backward direction. This implies that the system exhibits a well-defined hysteresis. In the case of forward continuation, we observe that the transition does not take place abruptly, rather it is in steps suggestive of cluster formation. This observation suggests that all the nodes do not join the synchronous component at the same value of the coupling. Instead, they perform a cascade of transition in joining the synchronous component.

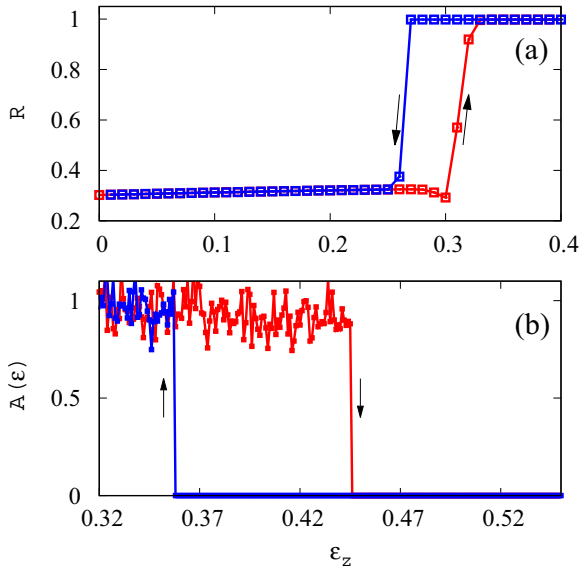

FIG. 1. Diagram showing the dynamical transitions in system Eqs. (1) and (2) with increasing coupling strength ε_z for $N = 500$. In (a), we plot the order parameter R showing transition from the desynchronized state to synchronization and in (b) we plot the order parameter $A(\varepsilon)$ that shows transition from an oscillatory state ($A(\varepsilon) \neq 0$) to a steady state ($A(\varepsilon) = 0$).

To explain the nature of the transition of the order parameter R [cf. Fig. 1(a)] in the forward direction, we observe that the dynamics on the nodes play an important role in the formation of clusters. Coupled Lorenz oscillators consist of distinct collective states corresponding to five coexisting attractors. We denote these by A_0, A_+, A_-, A_{i^+}, A_{i^-} [41,43,44]. These attractors can be described by examining the projection of their dynamics in the (x, y) planes as shown in Fig. 2. For small coupling strengths, the dynamics is on a desynchronized A_0 attractor [shown in Fig. 2(a)], and hence the order parameter R has a small value. Near the transition point, i.e., at $\varepsilon_z \approx 0.3$, the coexisting attractors are A_- and A_+, as shown in

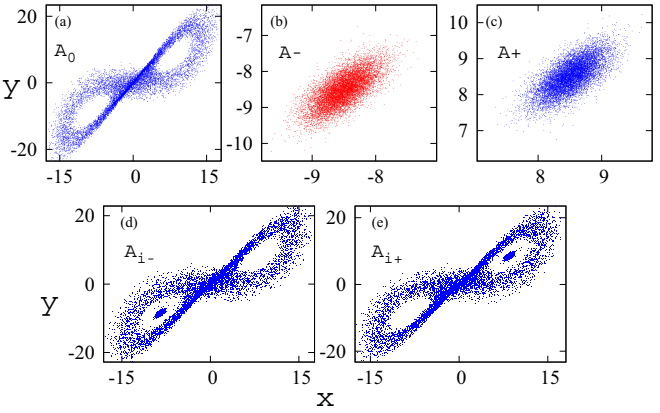

FIG. 2. Multistable attractors (a) A_0, (b) A_-, (c) A_+, (d) A_{i^-}, and (e) A_{i^+} observed in coupled Lorenz oscillators [Eqs. (1) and (2)] at coupling strength $\varepsilon_z = 0.3$.

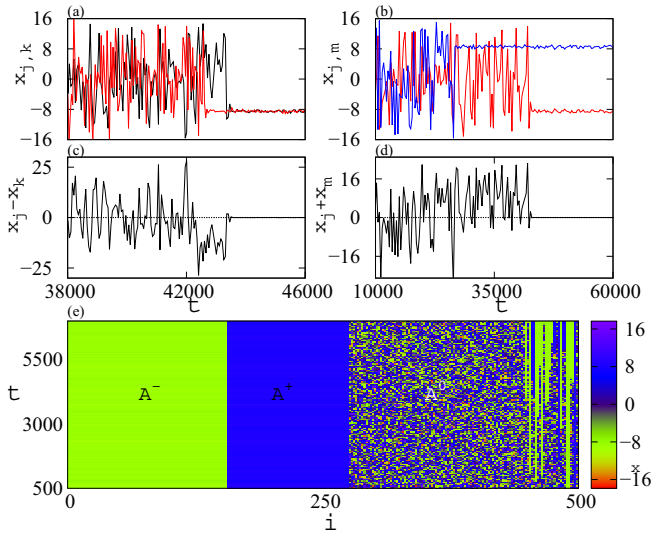

FIG. 3. Dynamics of the system given by Eqs. (1) and (2) at $\varepsilon_z = 0.3$ and $N = 500$. In (a), we plot the time series for any two nodes for $j = 121$ (red line) and $k = 403$ (black line) showing intermittent synchrony which is confirmed in (c) where we plot the time series of the difference variables $x_j - x_k$. The intermittent antisynchrony is observed in the nodes $j = 121$ (red line) and $m = 204$ (blue line) for which we plot in (b) the time series of the x variables of the two nodes and in (d) the time series of $x_j + x_m$. Further the dynamics of the ensemble is described by plotting (e) the space time evolution of the ensemble, where the green region represents A_- attractors, the blue region corresponds to A_+ attractors. The region for $i \gtrsim 260$ shows the A_0 and A_i attractors.

Figs. 2(b) and 2(c), respectively, where the dynamics is either in phase or antiphase. Further, we also observe that oscillators may jump from one attractor to another and the dynamics is not confined to a given attractor. These attractors are denoted by A_i, where the subscript i denotes the intermittent dynamics. In Figs. 2(d) and 2(e), we plot A_{i^-} and A_{i^+} dynamics, respectively. In $A_{i^{-(+)}}$ dynamics, the oscillator is on A_0 type and then it jumps to $A_{-(+)}$ attractor. These coexisting attractors occur for the coupling values very close to the transition point ($\varepsilon_z \approx 0.3$), where the dynamics is intermittently synchronized (or desynchronized) [43,45]. Thus, as a result of intermittent synchrony (antisynchrony), the order parameter R changes in small steps as the coupling strength is increased [Fig. 1(a)].

To understand the dynamics at the individual node level, we plot the time series and space-time plots for the ensemble in Fig. 3. The time series for two representative oscillators showing intermittent synchrony and antisynchrony is shown in Figs. 3(a) and 3(b), respectively. In Fig. 3(a), we plot the time series of two oscillators x_j (red line) and x_k (black line) for $j = 121$ and $k = 403$, each showing A_{i^-} dynamics. The two oscillators exhibit intermittent synchrony as shown in Fig. 3(c), where we plot the time evolution of the difference of coordinates $x_j - x_k$. Time evolution of the oscillators showing intermittent antisynchrony is shown in Fig. 3(b) where we plot the time series of two oscillators x_j (red line) and x_m (blue line) for $j = 121$ and $m = 204$ for which the orbits asymptote to A_+ and A_- dynamics, respectively. We observe that the oscillators show intermittent antisynchrony, which can also be seen in Fig. 3(d) where the time evolution of the sum of coordinates $x_j + x_m$ is plotted. The space-time plot near the transition point is shown in Fig. 3(e), which suggests that the dynamics is an intermittent chimera state. In the present case, the sequence of the oscillators is not important in the sense that a given oscillator may go to any of the available attractors depending upon the initial condition. Thus, while plotting Fig. 3(e), we reorder the indices of the oscillators in such a way that the oscillators going to the same attractor are grouped together. Thus, we note that the dynamics of some of the oscillators hop between attractors, resulting in intermittent synchrony (antisynchrony) and desynchrony and the overall dynamics is an intermittent chimera state [44,46]. If the coupling is increased beyond the transition point $\varepsilon_z > 0.3$, we observe that all the oscillators go to either A_- or A_+ attractors.

B. Transition to death ($\varepsilon_z \geqslant 0.35$)

Further, for large values of ε_z ($\varepsilon_z \geqslant 0.35$), we plot the order parameter $A(\varepsilon)$ versus ε_z in both the forward and the backward continuations in Fig. 1(b). We note that the forward and backward transition points are different, resulting in a hysteresis. The system makes a transition to amplitude death through the stabilization of the fixed point. Thus, the system of coupled oscillators continue to show global amplitude death if the coupling is increased in the forward direction. If we reduce the coupling in the backward direction, the system, which was initially in the steady state, will make an abrupt transition to an oscillatory regime where all the oscillators are synchronized. Such behavior where the system makes a transition from the oscillatory state to death with increasing coupling strength and vice versa when the coupling strength is decreased is termed ED [8].

C. Parameter space

To have a comprehensive understanding of the collective behavior of coupled oscillators, we demonstrate various dynamical states in the $\varepsilon_z - \gamma_n$ parameter space at $\gamma_h = 30$ using both the forward and backward continuations of ε_z. In Fig. 4, we show various spatiotemporal dynamics described by different grey tones (color online). These regimes can be demonstrated as the desynchronized state (DS), synchronized state (S), and amplitude death (D). The region for the chimera state is shown in red color. HA_1 represents the hysteresis area corresponding to the ES whereas HA_2 and HA_3 represents the hysteresis area corresponding to ED. Blue line indicates the parameter values for which we plot the order parameters R and $A(\varepsilon)$ in Figs. 1(a) and 1(b), respectively. The black lines mark the boundary of the hysteresis regions.

Consider the bifurcation parameter in the range $\gamma_n \in [24.06, 24.74]$, which is the region of subcritical Hopf bifurcation. In this region, there are three coexisting attractors consisting of two symmetric fixed points and the strange chaotic attractor. In this regime, the collective dynamics of the system is a chimera state for small values of ε_z depicted by red in Fig. 4. As the value of ε_z increases, we observe that the collective dynamics is synchronized and is indicated by the yellow region marked by S. If ε_z is increased further, we observe that all the oscillators are stabilized to a steady state or

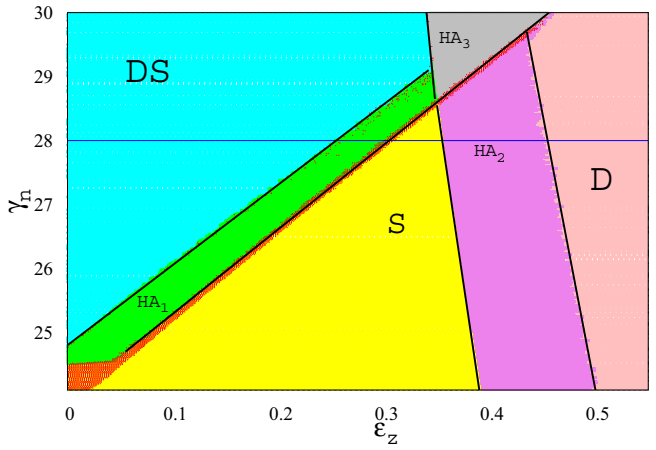

FIG. 4. Parameter space $\varepsilon_z - \gamma_n$ at $\gamma_h = 30$ and $N = 100$ for the system given by Eqs. (1) and (2). DS indicates the region for which we have desynchorinzed state (cyan), S denotes the synchronized state (yellow), and D implies the region of amplitude death (pink). Hysteresis regions corresponding to ES and ED are denoted by HA_1 (green) and HA_2 (purple) respectively. HA_3 (grey) is the hysteresis area corresponding to the transition from DS to amplitude death. The region shown in red is the region of chimera states. Blue line indicates the parameter value for which we have plotted the order parameters R and $A(\varepsilon)$ in Fig. 1, while the black lines mark the boundaries of the hysteresis regions.

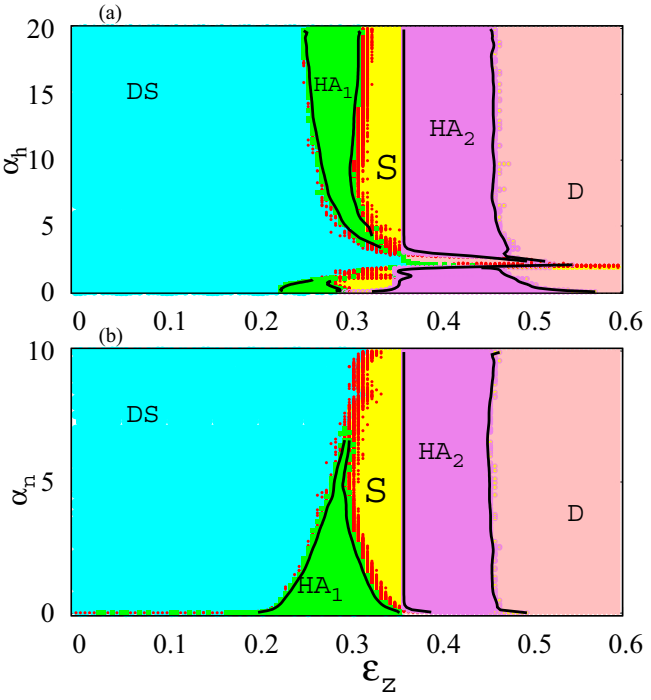

FIG. 5. For an ensemble of $N = 100$ oscillators, we plot the parameter space for the system given by Eqs. (1) and (2). We plot the parameter space (a) $\varepsilon_z - \alpha_h$ for $\alpha_n = 2$ and (b) $\varepsilon_z - \alpha_n$ at $\alpha_h = 20$. DS indicates the desynchronized region (cyan), S denotes the synchronized region (yellow) and the region marked in red color indicates chimera states. D denotes the region of amplitude death (pink). HA_1 (green) and HA_2 (purple) are the hysteresis areas corresponding to ES and ED, respectively, with their boundaries marked by the black lines.

amplitude death shown by orange (region D). Here we observe hysteresis area HA_2 in the parameter plane, indicating that the forward and backward transition points are different, resulting in explosive death.

Above the Hopf bifurcation, where $\gamma_n \in [25,29]$, the system is initially desynchronized (cyan), indicated by DS, for small values of ε_z. As the value of ε_z increases, the system makes transition to a synchronized state denoted by S. Note that this transition from desynchrony to synchrony is an irreversible transition accompanied by hysteresis denoted by HA_1. This is an instance of ES because the transition is discontinuous in nature and is associated with a hysteresis. On increasing ε_z further, the system shows explosive death where an abrupt transition to steady state, shown in pink (region D), takes place and the associated hysteresis area is denoted by HA_2. Furthermore, when $\gamma_n > 29$, we observe that the system makes an irreversible transition from desynchronized state (DS) to the steady state (D), having hysteresis area HA_3.

We note that the nature of the transition in this system crucially depends on the timescale parameters α_n and α_h. Thus, the investigation of the nature of the transition in the $\varepsilon_z - \alpha_{n(h)}$ parameter space leads to a more thorough understanding of the phenomena. Figures 5(a) and 5(b) show the parameter space $\varepsilon_z - \alpha_n$ at $\alpha_h = 20$ and $\varepsilon_z - \alpha_h$ at $\alpha_n = 2$, respectively, where we plot the order parameter R in the forward and the backward directions. The distinct areas are represented as DS, S, and D as already described in Fig. 4. Regions HA_1 and HA_2 denote hysteresis areas corresponding to ES and ED, respectively.

In Fig. 5(a), we plot the $\varepsilon_z - \alpha_h$ parameter space for $\alpha_n = 2$ and observe that at $\varepsilon_z \leqslant 0.2$, for all values of α_h the collective dynamics is a desynchronized state denoted by DS. When $\alpha_h = \alpha_n = 2$, the system will be in desynchronized state (DS) for smaller values of ε_z and the chimera state (red color) appears as ε_z increases. For this value of α_h, we do not observe any phase transition. However, for $\alpha_h \neq \alpha_n$, the system makes an abrupt transition to synchrony, namely, ES as the value of ε_z increases. We denote the hysteresis area by HA_1. Note that HA_1 increases on increasing α_h. On increasing ε_z further ($\varepsilon_z \geqslant 0.35$), we note that the system finally makes a discontinous transition to the steady state. The associated hysteresis area for this case is denoted by HA_2.

The parameter space $\varepsilon_z - \alpha_n$ for $\alpha_h = 20$ is plotted in Fig. 5(b). We note that for small values of ε_z ($\varepsilon_z \leqslant 0.2$) the system dynamics is desynchronized (DS). If α_n increases, the system dynamics shows an irreversible transition to synchrony, with the hysteresis area denoted by HA_1. Further, on increasing α_n the hysteresis area (HA_1) disappears for $\alpha_n > 5$, where the system makes transition from DS to S continuously. In this regime, the system shows a second-order transition to phase synchronization. For larger values of ε_z, we again observe an abrupt transition from synchronized states to death, namely, ED. The hysteresis area associated with the explosive transition to death is denoted by HA_2.

D. Stability of the states

To understand the stability of the synchronized states, we calculate the master stability function (MSF) for the system.

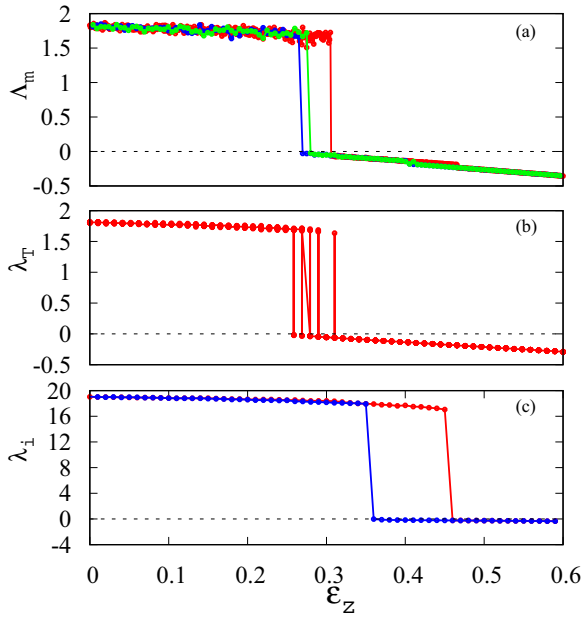

FIG. 6. Stability of various states for the system given by Eqs. (1) and (2). In (a), we plot the variation of the master stability function (Λ_m) for three attractors A_0, A_-, A_+; (b) transversal Lyapunov exponent (λ_T) for two oscillators for 20 initial conditions; and (c) largest Lyapunov exponent (λ_i) for the forward (red line) and backward (blue) continuations.

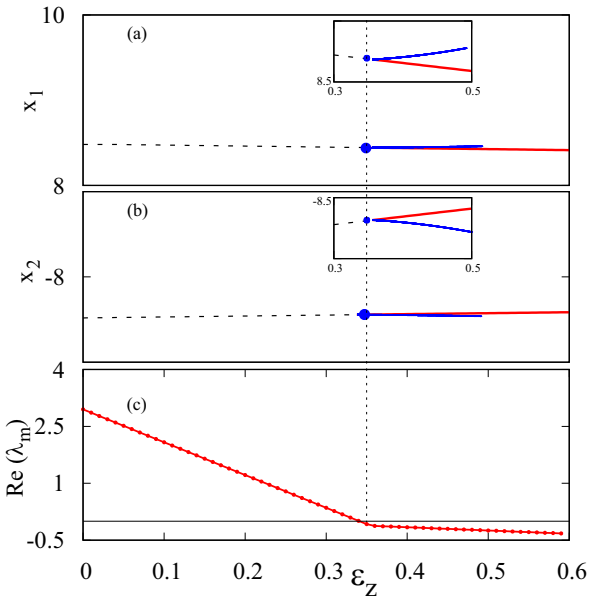

FIG. 7. The one parameter bifurcation diagram corresponding to the fixed points (a) $P_+ = (x_+^*, y_+^*, z_+^*)$ and (b) $P_- = (x_-^*, y_-^*, z_-^*)$. The dashed line represents the unstable steady state whereas the solid red and blue lines represent stable steady state and periodic solutions, respectively. The Hopf bifurcation point is marked as HB and is denoted by a blue dot. In (c), we plot the real part of the eigenvalue [Re(λ_m)] of the Jacobain matrix Eq. (C1).

It was shown that the MSF (Λ_m) describes the stability of the synchronization manifolds for the N coupled oscillators [47,48]. However, in case of multistable systems, it is important to calculate the MSF for each attractor [49]. Thus, to understand the linear stability of the synchronized states we calculate the MSF for Eqs. (1) and (2) for each coexisting attractors by setting $\varepsilon_x = \varepsilon_y = 0$. The procedure to calculate the MSF has been outlined in Appendix A. As shown in Fig. 6(a), we plot the three curves corresponding to the attractors, namely, A_0, A_-, and A_+. We notice that for each attractor, the MSF (Λ_m) crosses the zero line for three different values of ε_z. The synchronized states corresponding to $A_\pm$ attractors become stable for smaller values of the coupling strengths (green and blue curves) while for A_0 the synchronized state becomes stable as ε_z increases.

To understand the dynamics at the level of two oscillators, we consider two nodes coupled to a hub and study the growth of perturbations corresponding to the transversal manifold by calculating the transversal Lyapunov exponents (TLEs) denoted by λ_T. The method to calculate the TLE has been described in Appendix B. If the Lyapunov exponent corresponding to the transversal manifold, namely, the TLE (λ_T) is positive, the perturbations will grow and the two nodes will be desynchronized. However, if λ_T is negative, the perturbations will die out and the synchronized state is stable. As shown in Fig. 6(b), λ_T becomes negative in the region of transition, indicating that the two nodes are in complete synchronization. Fluctuations in the values of TLE near the transition region is due to the multistability, wherein we observe multiple coexisting synchronized and desynchronized attractors. If for a given set of initial conditions, the dynamics is on $A_\pm$ attractors, the TLE is negative since the $A_\pm$ attractors are synchronized. However, if the dynamics is on the A_0 attractor the oscillators are desynchronized and the TLE is positive. Further, we plot the largest Lyapunov exponent (λ_i) in Fig. 6(c) to characterize these transitions. We observe that the largest LE changes abruptly at the forward and the backward transition points. This implies that the coupled system is in a chaotic state before the transition.

In Figs. 7(a) and 7(b), we plot the bifurcation diagram for the system of two nodes using XPPAUT software [50] corresponding to the fixed pints $P_+ = (x_+^*, y_+^*, z_+^*)$ and $P_- = (x_-^*, y_-^*, z_-^*)$, respectively. We observe that the unstable steady state of the system, denoted by the dashed line, is stabilized via Hopf bifurcation (HB) and the final state of the system is a stable steady state shown by red line. Further, this is verified by the stability analysis of the system Eqs. (1) and (2) having fixed points $x^* = y^* = \pm\sqrt{\beta(\gamma-1)}$ and $z^* = \gamma - 1$. Since the nodes are identical and are interacting with the hub with equal coupling strength, we can study the stability of the fixed points by calculating the eigenvalues of the Jacobian given by Eq. (C1). For the symmetry-preserving case, the coupling is present only in the z variable, namely, $\varepsilon_x = \varepsilon_y = 0$, $\varepsilon_z \neq 0$. In this setting, we plot the eigenvalues of the Jacobian Eq. (C1) in Fig. 7(c). As shown, the largest eigenvalue shows a transition at a point where the system makes an explosive transition to death. This matches well with the HB point in Figs. 7(a) and 7(b), respectively.

IV. TRANSITIONS WITH BROKEN SYMMETRY

We study the dynamics in the presence of symmetry breaking coupling by considering a star network of coupled Lorenz

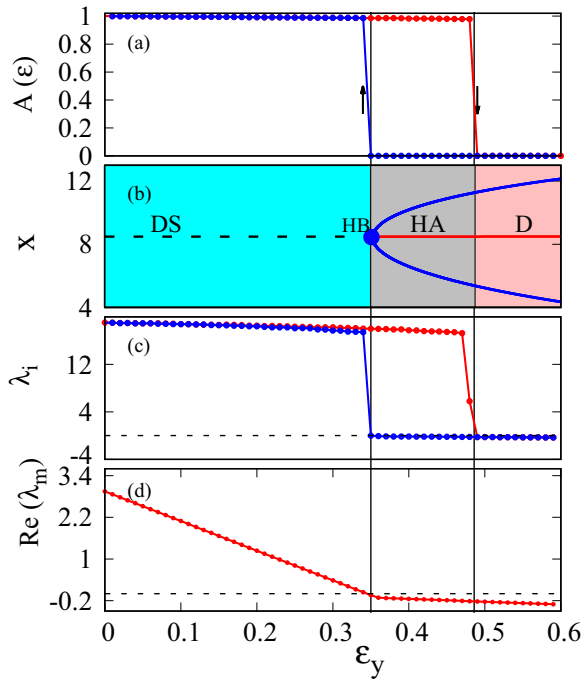

FIG. 8. Dynamical transitions for the system given by Eqs. (1) and (2) for the symmetry-broken case. We plot in (a) the variation of the order parameter $A(\varepsilon)$ as a function of ε_y showing explosive death for $N = 500$ and (b) the bifurcation diagram for the case of two coupled oscillators using XPPAUT software, where HB denotes the Hopf bifurcation. The dashed line represents the unstable steady state whereas the solid red and blue lines represent stable steady state and periodic solutions, respectively. Since the transitions do not depend on γ_n, we show the entire parameter space as a function of ε_y for $\gamma_h = 30$, showing desynchorinzed state (DS) in cyan, hysteresis area (HA) (grey), and the region of amplitude death (D) (pink). In (c), we plot the largest Lyapunov exponent (λ_i) for the forward (red line) and backward (blue line) continuations. In (d), we plot the real part of the largest eigenvalue [Re(λ_m)] of the Jacobian [Eq. (C1)] for the symmetry-breaking case.

oscillators as described in Eqs. (1) and (2). In this scenario, the coupling is done such that $\varepsilon_y \neq 0$ and $\varepsilon_x = \varepsilon_z = 0$. To explore the dynamics of the coupled oscillators, we plot the order parameter $A(\varepsilon)$ defined in Eqs. (4) and (5). $A(\varepsilon) > 0$ denotes the oscillatory state whereas $A(\varepsilon) = 0$ implies death or suppression of oscillations. For $N = 500$ oscillators, we calculate $A(\varepsilon)$ by increasing the coupling ε_y adiabatically in the forward direction up to a maximum value as shown in Fig. 8(a). Similarly, in the backward direction we start from the maximum value of ε_y and then decrease ε_y adiabatically until $\varepsilon_y = 0$. In the forward direction, we observe a discontinuous jump in the order parameter which becomes zero and the oscillations are suppressed. Similarly, in the backward case, the order parameter $A(\varepsilon)$ makes an abrupt transition to a nonzero value. We observe that the forward and backward transition points are different, indicative of a well-defined hysteresis. This is suggestive of an explosive transition to death, namely, explosive death. As opposed to the symmetry-preserving case, here we do not observe any instance of synchronization.

In Fig. 8(b), we plot the bifurcation diagram for the system of two nodes depicting bifurcations taking place in the system using XPPAUT software [50]. We observe that the fixed points of the system are stabilized via HB and the final state of the system is a steady state. We also observe that the system dynamics is independent of the system parameter γ_n and depends only on the coupling strength ε_y. Therefore, in Fig. 8(b), we show various regions as a function of ε_y for a fixed value of $\gamma_h = 30$. Our findings indicate that the system is desynchronized if the coupling strength $\varepsilon_y < 0.35$ for all the values of γ_n and this region is denoted by DS (cyan). The region $0.35 < \varepsilon_y < 0.45$ shows the hysteresis area (HA) (grey) and, finally, for $\varepsilon_y > 0.45$, the system dynamics is a steady state denoted by D (pink). To corroborate further, we plot the variation in the largest Lyapunov exponent (λ_i) of the system as shown in Fig. 8(c), for the forward (red line) and the backward (blue line) transition points. The largest LE changes its sign abruptly at the forward and backward transition points. This shows that the coupled system is in a chaotic state before it makes a transition to the steady state. To understand the transition to amplitude death, we investigate the stability of the system [Eqs. (1) and (2)] having fixed points $x^* = y^* = \pm\sqrt{\beta(\gamma - 1)}$ and $z^* = \gamma - 1$. Since this is the symmetry-breaking case, the coupling is present only in the y variable, namely, $\varepsilon_x = \varepsilon_z = 0$, $\varepsilon_y \neq 0$. As discussed earlier, we can study the stability of the fixed points by calculating the eigenvalues of the Jacobian given by Eq. (C1). We observe that when the system makes a transition to amplitude death, the real part of the largest eigenvalue Re(λ_m) becomes negative, as shown in Fig. 8(d). This transition point matches well with the numerically predicted values and the Hopf bifurcation point.

V. CONCLUSION AND DISCUSSION

We study the dynamics of coupled Lorenz oscillators on a star network configuration. The oscillators on the hub and the nodes have varying timescales. This is done to incorporate degree frequency correlation in the system. Our interest is to understand the dynamical consequences of couplings such that the symmetry is either preserved or destroyed. Under the influence of symmetry preserving coupling, the system shows consecutive explosive transitions having distinct hysteresis loops. The first of these transitions is an explosive synchronization where the system makes a first order transition from desynchronized state to the synchronized state. The order parameter changes in steps because of the formation of intermediate clusters. The formation of clusters takes place as a result of intermittent synchrony and antisynchrony amongst the nodes. Near the transition point, we also note that the dynamics is an intermittent chimera state. The stability of these states is studied by calculating the master stability function for the coexisting attractors individually and the largest LE. Further, at the level of two oscillators, we verify this transition with the help of transversal LE. If the coupling strength is increased further, we note that a second transition takes place. In this case, the system shows an abrupt transition from synchronized oscillatory state to steady state namely the explosive death. This transition point is studied with the help of local stability analysis. However, if the symmetry is broken,

we observe that there is an abrupt transition to death namely ED. This happens in the system as a result of the coexistence of stable oscillatory solutions and stable steady-state solutions across a wide range of parameter values. This transition is again verified with the help of stability analysis and the largest LE.

Thus, we give evidence that disparate abrupt transitions may occur as a result of the timescale variations in a system of coupled chaotic oscillators. One can tune the timescale variation parameters to control the hysteresis area and the nature of transitions. We show that the region of hysteresis is governed by the interplay of the timescale variations and the coupling strength. The master stability function, Lyapunov exponents, bifurcation diagram, and the linear stability analysis are found to be in good agreement with the numerical results. The results obtained in this paper show that it is possible to observe explosive transitions in coupled chaotic systems along with distinct multistable states. Additionally, the proposed study opens numerous questions and has wide applicability. The Lorenz system is a paradigmatic model to study the dynamical properties of chaotic systems. Since the system exhibits very rich and interesting dynamics for various values of the control parameter γ, it will be interesting to extend this study for different regimes and to various network topologies.

APPENDIX A: THE MASTER STABILITY FUNCTION

To classify and understand the stability conditions for different states, we study the MSF for the system as described in Ref. [47]. Consider a typical network for N coupled oscillators described by

$$\dot{\mathbf{x}}_i = \mathbf{F}(\mathbf{x}_i) - \varepsilon \sum_{j=1}^{N} G_{ij}\mathbf{H}(\mathbf{x}_j), \tag{A1}$$

where $\mathbf{F}$ represents the dynamics of the uncoupled system, $\mathbf{H}$ and $\mathbf{G}$ are the matrices that specify the coupling in the network with their matrix elements denoted by H_{ij} and G_{ij}, respectively. The coupling strength corresponding to the coupled variables is denoted by ε. Matrix $\mathbf{G}$ satisfies the condition $\sum_{j=1}^{N} G_{ij} = 0$ for any i. For the synchronized state given by $\mathbf{x}_1 = \mathbf{x}_2 = \cdots = \mathbf{x}_N = \mathbf{s}$, the variational equation governing the time evolution of the infinitesimal vectors about $\mathbf{s}$ is given by

$$\delta\dot{\mathbf{x}} = \mathbf{DF}(\mathbf{s}).\delta\mathbf{x}_i - \varepsilon \sum_{j=1}^{N} G_{ij}\mathbf{DH}(\mathbf{s}).\delta\mathbf{x}_j, \tag{A2}$$

where $\delta\mathbf{x}_i = \mathbf{x}_i - \mathbf{s}$, $\mathbf{DF}(\mathbf{s})$ and $\mathbf{DH}(\mathbf{s})$ are the Jacobian matrices corresponding to the vector eigenfunctions evaluated at $\mathbf{s}(t)$. Consider the transformation $\delta\mathbf{y} = \mathbf{Q}^{-1}\delta\mathbf{x}$, where the columns of matrix Q are given by the set of eigenvectors of $\mathbf{G}$, resulting in the generic form for decoupled blocks given by

$$\delta\dot{\mathbf{y}} = [\mathbf{DF}(\mathbf{s}) - K\mathbf{DH}(\mathbf{s})].\delta\mathbf{y}_j, \tag{A3}$$

where K is the normalized coupling parameter. The largest LE (Λ_m) of Eq. (A3) is the MSF for the system. The procedure to calculate the Lyapunov exponent has been outlined in Refs. [48,51].

APPENDIX B: TRANSVERSAL LYAPUNOV EXPONENT

Consider a pair of identical Lorenz oscillator nodes coupled to a hub in such a way that the coupling preserves symmetry. The equations of motion for the dynamics on the nodes is given by

$$\begin{aligned}
\dot{x}_1 &= \alpha_n[\rho(y_1 - x_1)],\\
\dot{y}_1 &= \alpha_n[\gamma_n x_1 - y_1 - x_1 z_1],\\
\dot{z}_1 &= \alpha_n[x_1 y_1 - \beta z_1 + \varepsilon_z(z_h - z_1)]\\
\dot{x}_2 &= \alpha_n[\rho(y_2 - x_2)],\\
\dot{y}_2 &= \alpha_n[\gamma_n x_2 - y_2 - x_2 z_2],\\
\dot{z}_2 &= \alpha_n[x_2 y_2 - \beta z_2 + \varepsilon_z(z_h - z_2)],
\end{aligned} \tag{B1}$$

and the dynamics of the hub is given by

$$\begin{aligned}
\dot{x}_h &= \alpha_h[\rho(y_h - x_h)],\\
\dot{y}_h &= \alpha_h[\gamma_h x_h - y_h - x_h z_h],\\
\dot{z}_h &= \alpha_h[x_h y_h - \beta z_h + \frac{\varepsilon_z}{2}\{(z_1 - z_h) + (z_2 - z_h)\}].
\end{aligned} \tag{B2}$$

The nodes are diffusively coupled to the hub through the z variable and by adjusting the strength ε_z, the two nodes can be made to synchronize. The stability of the synchronization manifold can be determined by transforming the variables in the following way [52]:

$$\begin{aligned}
x &= \frac{x_2 - x_1}{2};\ y = \frac{y_2 - y_1}{2};\ z = \frac{z_2 - z_1}{2},\\
X &= \frac{x_2 + x_1}{2};\ Y = \frac{y_2 + y_1}{2};\ Z = \frac{z_2 + z_1}{2}.
\end{aligned} \tag{B3}$$

Further, we rewrite Eq. (B1) in terms of the transformed variables defined in Eq. (B3) and obtain

$$\begin{aligned}
\dot{x} &= \alpha_n[\rho(y - x)],\\
\dot{y} &= \alpha_n[\gamma_n x - y - (Xz + Zx)],\\
\dot{z} &= \alpha_n[-(\beta + \varepsilon_z)z + Xy + Yx],\\
\dot{X} &= \alpha_n[\rho(Y - X)],\\
\dot{Y} &= \alpha_n[\gamma_n X - Y - (XZ + xz)],\\
\dot{Z} &= \alpha_n[-\beta Z + XY + xy + \varepsilon_z z_h - \varepsilon_z Z].
\end{aligned} \tag{B4}$$

The transformed system is thus expressed in the new set of coordinates where (X, Y, Z) are on the synchronization manifold while (x, y, z) are the coordinates corresponding to the transverse manifold. To understand the growth or decay of perturbations transverse to the synchronization manifold, we calculate the TLE for the variational equations of x, y, z at $x = y = z = 0$ [39,53], given by

$$\begin{aligned}
\delta\dot{x} &= \alpha_n[\rho(\delta y - \delta x)],\\
\delta\dot{y} &= \alpha_n[\gamma_n\delta x - \delta y - (X\delta z + Z\delta x)],\\
\delta\dot{z} &= \alpha_n[-(\beta + \varepsilon_z)\delta z + X\delta y + Y\delta x].
\end{aligned} \tag{B5}$$

Here, δx, δy, and δz respectively, are the perturbations for the variables x, y, and z in the transversal manifold. When the largest TLE is positive, then perturbations will grow and the system is in the desynchronized state. However, if the

TLE is negative, the perturbations transverse to the synchronization manifold will die out and the system collapses onto the synchronization manifold, resulting in the synchronized state [52]. Numerically, these TLEs are obtained by means of the algorithm by Benettin *et al.* [51]. Here we consider the basis vectors to derive tangential dynamics using Jacobian and Gram-Schmidt normalization of Eq. (B5). We have calculated TLE using the following equation:

$$\lambda_T = \frac{1}{n_{\rm ev}\tau}\sum_{k=1}^{n_{\rm ev}} \ln\left|\left|{v_j}^k\right|\right|, \tag{B6}$$

where $\tau = 0.001$ is the time step, $n_{\rm ev} = 10^6$ is the evolution time, $j = 1, 2, 3$ and v_j are the orthonormal basis vectors [54].

APPENDIX C: LINEAR STABILITY ANALYSIS

The transition points corresponding to the ED in the system can be calculated by performing the stability analysis of the steady state of the nodes, since the stability of these states will get modified in the presence of coupling. Note that when the system is in the steady state, each node has a fixed point given by $x^* = y^* = \pm\sqrt{\beta(\gamma-1)}$ and $z^* = \gamma - 1$. For these fixed points, we calculate the eigenvalues λ_m of a $3N \times 3N$ Jacobian matrix corresponding to the nodes [see Eq. (1)] that evolve under the influence of a hub. Since all nodes evolve to the same steady state, one needs to calculate the eigenvalues of the following Jacobian:

$$\mathbf{J} = \begin{pmatrix} \alpha_n(-\rho-\varepsilon_x) & \alpha_n\rho & 0 & \alpha_n\varepsilon_x & 0 & 0 \\ \alpha_n(\gamma_n - z^*) & \alpha_n(-1-\varepsilon_y) & -\alpha_n x^* & 0 & \alpha_n\varepsilon_y & 0 \\ \alpha_n y^* & \alpha_n x^* & \alpha_n(-\beta-\varepsilon_z) & 0 & 0 & \alpha_n\varepsilon_z \\ \alpha_h\varepsilon_x & 0 & 0 & \alpha_h(-\rho-\varepsilon_x) & \alpha_h\rho & 0 \\ 0 & \alpha_h\varepsilon_y & 0 & \alpha_h(\gamma_h - z^*) & \alpha_h(-1-\varepsilon_y) & -\alpha_h x^* \\ 0 & 0 & \alpha_h\varepsilon_z & \alpha_h y^* & \alpha_h x^* & \alpha_h(-\beta-\varepsilon_z) \end{pmatrix}. \tag{C1}$$

[1] A. Pikovsky, M. Rosenblum, and J. Kurths, *Synchronisation: A Universal Concept in Nonlinear Science* (Cambridge University Press, Cambridge, 2001).
[2] Y. Kuramoto and D. Battogtokh, Nonlinear Phenom. Complex Syst. **5**, 380 (2002).
[3] S. H. Strogatz, *Sync: The Emerging Science of Spontaneous Order* (Hyperion, New York, 2003).
[4] J. Gómez-Gardeñes, S. Gómez, A. Arenas, and Y. Moreno, Phys. Rev. Lett. **106**, 128701 (2011).
[5] H. Bi, X. Hu, X. Zhang, Y. Zou, Z. Liu, and S. Guan, Europhys. Lett. **108**, 50003 (2014).
[6] U. K. Verma, A. Sharma, N. K. Kamal, and M. D. Shrimali, Chaos **29**, 063127 (2019).
[7] U. K. Verma, S. S. Chaurasia, and S. Sinha, Phys. Rev. E **100**, 032203 (2019).
[8] K. Sathiyadevi, D. Premraj, T. Banerjee, and M. Lakshmanan, Phys. Rev. E **106**, 024215 (2022).
[9] O. E. Omel'chenko and M. Wolfrum, Phys. Rev. Lett. **109**, 164101 (2012).
[10] H.-A. Tanaka, A. J. Lichtenberg, and S. Oishi, Phys. Rev. Lett. **78**, 2104 (1997).
[11] T. K. DM. Peron and F. A. Rodrigues, Phys. Rev. E **86**, 016102 (2012).
[12] S. Boccaletti, V. Latora, Y. Moreno, M. Chavez, and D.-U. Hwang, Phys. Rep. **424**, 175 (2006).
[13] B. M. Adhikari, C. M. Epstein, and M. Dhamala, Phys. Rev. E **88**, 030701(R) (2013).
[14] M. Kim, R. E. Harris, A. F. DaSilva, and U. Lee, Front. Comput. Neurosci. **16**, 815099 (2022).
[15] S. V. Buldyrev, R. Parshani, G. Paul, H. E. Stanley, and S. Havlin, Nature (London) **464**, 1025 (2010).
[16] B. A. Huberman and R. M. Lukose, Science **277**, 535 (1997).
[17] P. Ji, T. K. DM. Peron, P. J. Menck, F. A. Rodrigues, and J. Kurths, Phys. Rev. Lett. **110**, 218701 (2013).
[18] X. Zhang, S. Boccaletti, S. Guan, and Z. Liu, Phys. Rev. Lett. **114**, 038701 (2015).
[19] M. M. Danziger, I. Bonamassa, S. Boccaletti, and S. Havlin, Nat. Phys. **15**, 178 (2019).
[20] A. D. Kachhvah and S. Jalan, Europhys. Lett. **119**, 60005 (2017).
[21] S. Jalan, V. Rathore, A. D. Kachhvah, and A. Yadav, Phys. Rev. E **99**, 062305 (2019).
[22] T. Wu, S. Huo, K. Alfaro-Bittner, S. Boccaletti, and Z. Liu, Phys. Rev. Res. **4**, 033009 (2022).
[23] V. Vlasov, Y. Zou, and T. Pereira, Phys. Rev. E **92**, 012904 (2015).
[24] X. Zhang, X. Hu, J. Kurths, and Z. Liu, Phys. Rev. E **88**, 010802(R) (2013).
[25] B. C. Coutinho, A. V. Goltsev, S. N. Dorogovtsev, and J. F. F. Mendes, Phys. Rev. E **87**, 032106 (2013).
[26] I. Leyva, R. Sevilla-Escoboza, J. M. Buldú, I. Sendiñ-Nadal, J. Gómez-Gardenes, A. Arenas, Y. Moreno, S. Gomez, R. Jaimes-Reátegui, and S. Boccaletti, Phys. Rev. Lett. **108**, 168702 (2012).
[27] H. Chen, G. He, F. Huang, C. Shen, and Z. Hou, Chaos **23**, 033124 (2013).
[28] B. R. R. Boaretto, R. C. Budzinski, T. L. Prado, and S. R. Lopes, Phys. Rev. E **100**, 052301 (2019).
[29] C. Sparrow, *The Lorenz Equations: Bifurcations, Chaos, and Strange Attractors* (Springer, New York, 1982).
[30] E. N. Lorenz, J. Atmos. Sci. **20**, 130 (1963).
[31] H. Haken, Phys. Lett. A **53**, 77 (1975).
[32] E. Knobloch, Phys. Lett. A **82**, 439 (1981);

[33] A. E. Motter, S. A. Myers, M. Anghel, and T. Nishikawa, Nat. Phys. **9**, 191 (2013).
[34] L. Cuadra, S. Salcedo-Sanz, J. Del Ser, S. Jimènez-Fernàndez, and Z. W. Geem, Energies **8**, 9211 (2015).
[35] R. Carareto, M. S. Baptista, and C. Grebogi, Commun. Nonlinear Sci. Numer. Simul. **18**, 1035 (2013).
[36] R. S. Pinto and A. Saa, Phys. Rev. E **91**, 022818 (2015).
[37] M. Brede, Phys. Lett. A **372**, 2618 (2008).
[38] K. Pyragas, Phys. Rev. E **54**, R4508 (1996).
[39] S. Camargo, R. L. Viana, and C. Anteneodo, Phys. Rev. E **85**, 036207 (2012).
[40] S. R. Ujjwal, N. Punetha, M. Agarwal, R. Ramaswamy, and A. Prasad, Chaos **26**, 063111 (2016).
[41] S. R. Ujjwal, N. Punetha, A. Prasad, and R. Ramaswamy, Phys. Rev. E **95**, 032203 (2017).
[42] M. Agrawal, A. Prasad, and R. Ramaswamy, Phys. Rev. E **87**, 042909 (2013).
[43] A. A. Khatun, Y. A. Muthanna, N. Punetha, and H. H. Jafri, Phys. Rev. E **109**, 034208 (2024).
[44] A. A. Khatun, H. H. Jafri, and N. Punetha, Phys. Rev. E **103**, 042202 (2021).
[45] G. L. Baker, J. A. Blackburn, and H. J. T. Smith, Phys. Rev. Lett. **81**, 554 (1998).
[46] I. A. Shepelev, G. I. Strelkova, and V. S. Anishchenko, Chaos **28**, 063119 (2018).
[47] L. M. Pecora and T. L. Carroll, Phys. Rev. Lett. **80**, 2109 (1998).
[48] L. Huang, Q. Chen, Y. C. Lai, and L. M. Pecora, Phys. Rev. E **80**, 036204 (2009).
[49] R. Sevilla-Escoboza, J. M. Buldú, A. N. Pisarchik, S. Boccaletti, and R. Gutiérrez, Phys. Rev. E **91**, 032902 (2015).
[50] B. Ermentrout, *Simulating, Analyzing, and Animating Dynamical Systems: A Guide to XPPAUT for Researchers and Students (Software, Environments, Tools)* (SIAM, Philadelphia, 2002).
[51] G. Benettin, L. Galgani, A. Giorgilli, and J. Strelcyn, Meccanica **15**, 9 (1980).
[52] L. M. Pecora, T. L. Carroll, G. A. Johnson, D. J. Mar, and J. F. Heagy, Chaos **7**, 520 (1997).
[53] J. Aguirre, R. L. Viana, and M. A. F. Sanjuán, Rev. Mod. Phys. **81**, 333 (2009).
[54] M. Lakshmanan and S. Rajasekar, *Nonlinear Dynamics: Integrability, Chaos, and Patterns* (Springer-Verlag, Berlin, 2003).